Observations of Multiple Magnetic Islands in the Core of a Reversed Field Pinch

P. Franz,[1,2] L. Marrelli,[1,2] P. Piovesan,[1,2] B. E. Chapman,[3] P. Martin,[1,2] I. Predebon,[1,2] G. Spizzo,[1]
R. B. White,[4] and C. Xiao[3,5]

[1]*Consorzio RFX, Associazione EURATOM-ENEA sulla Fusione, Corso Stati Uniti, 4 35127 Padova, Italy**
[2]*Istituto Nazionale di Fisica della Materia, UdR Padova, Italy*
[3]*Department of Physics, University of Wisconsin—Madison, 1150 University Avenue, Madison, Wisconsin 53706, USA*
[4]*Plasma Physics Laboratory, Princeton University, P.O. Box 451, New Jersey 08540, USA*
[5]*Department of Physics and Engineering Physics, University of Saskatchewan, Saskatoon SK S7J 3J2, Canada*
(Received 8 July 2003; published 25 March 2004)

We describe in this Letter the first measurement of multiple islands in the core of a reversed field pinch (RFP). These islands appear with current profile modification leading to magnetic fluctuation reduction in the Madison symmetric torus RFP. Magnetic island widths decrease to an unprecedented level, reducing the overlap of adjacent islands and allowing distinct islands to appear. The structures are observed in multichord measurements of soft-x-ray emissivity. The soft-x-ray data is validated with Poincaré reconstructions of the magnetic field structure in the core.

DOI: 10.1103/PhysRevLett.92.125001 PACS numbers: 52.55.Lf, 52.25.Os, 52.55.Wq, 52.55.Tn

The ability of the reversed field pinch (RFP) configuration to confine plasma energy has for a long time been limited by a high level of magnetic turbulence. In a standard RFP discharge, magnetic instabilities (tearing modes) are present due to gradients in the current profile [1]. Experiments in which a pulsed electric field is applied at the plasma edge [the so-called pulsed poloidal current drive (PPCD)] [2–5] have allowed the transient reduction of magnetic turbulence. As a consequence, record improvements of the energy confinement time up to a factor of 10 have been achieved [3]. Recently, a population of very energetic electrons has been detected in the plasma core during PPCD and has been interpreted as a result of the substantial decrease of magnetic stochasticity in that region [6].

In this Letter we describe new soft-x-ray (SXR) measurements, which experimentally confirm that magnetic stochasticity is indeed strongly reduced. In particular, for the first time in a RFP, we report evidence of distinct magnetic islands, appearing as multiple SXR structures, during PPCD. While evidence of single structures in SXR emissivity, linked to a single dominant magnetic mode, has been found in various types of RFP plasma [7,8], multiple SXR structures occur only during PPCD, due to the dramatic decrease of magnetic fluctuation amplitudes, which reduces adjacent-islands overlap and, consequently, stochasticity. The reduction of stochasticity has been verified with the numerical reconstruction of the magnetic surface topology [9] using experimental measurements of magnetic perturbation amplitudes.

The key diagnostic for this study is a miniaturized pinhole SXR photocamera [10], which has been developed for Madison symmetric torus (MST) [11]. SXR emissivity is measured through a 16 μm-thick beryllium filter with a fanlike array of 12 lines of sight emanating from a pinhole at the plasma boundary. Because of magnetic mode rotation, analysis of the fluctuating component of the signals allows us to identify the presence of poloidally localized SXR structures. We analyzed a database of ≈ 50 discharges where modes were rotating and mode amplitudes were stationary for a sufficiently long time. We find that either one or two SXR structures can arise in the core during PPCD, depending on the Fourier spatial spectrum of the magnetic fluctuations (magnetic fluctuations are described by the poloidal and toroidal mode numbers, m and n, respectively).

Given its peculiar safety factor profile (shown in Fig. 1), the RFP magnetic fluctuation spectrum is dominated by $m = 1$ and $m = 0$ modes. The n spectrum is rich, as many resonant surfaces are simultaneously present in the plasma.

A clear separation of the cases with one SXR structure from those with two structures arises if we consider the magnetic fluctuation amplitude of the two innermost resonant modes. We plot in Fig. 2 the average amplitude of those modes, the $(m = 1, n = 6)$ and the $(1, 7)$, for a series of PPCD shots for which one or two structures, identified in the following as islands, are present. One

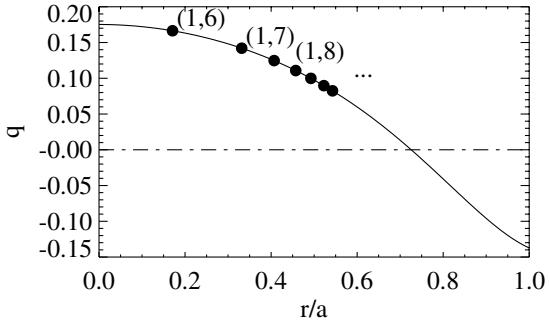

FIG. 1. Safety factor profile for an RFP discharge. Dots indicate the location of some $m = 1$ mode resonant surfaces.

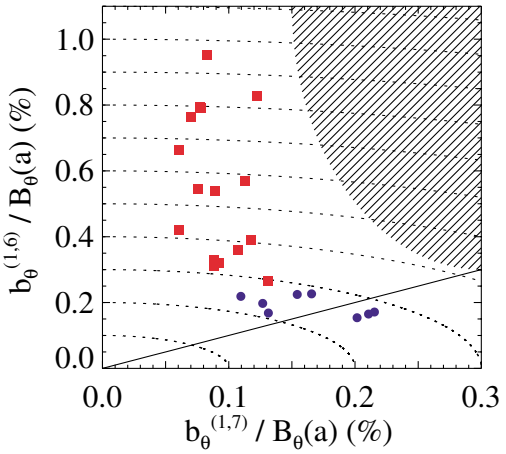

FIG. 2 (color). Normalized amplitude of the two innermost resonant $m = 1$ magnetic perturbations, $b_{\theta,(1,6)}$ vs $b_{\theta,(1,7)}$, for the PPCD shots in which one (red squares) or two (blue dots) SXR structures are present. Dashed lines represent constant mode energy (quadratic sum) contours. The grey area represents the region corresponding to standard discharges.

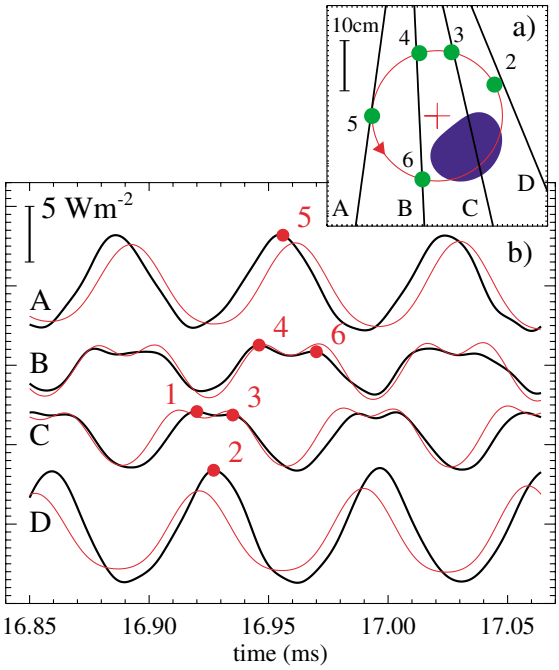

FIG. 3 (color). (a) Position of the simulated SXR hot region in a rotation period, in a poloidal cross section of MST. Four chords, relative to the SXR signals of panel (b), are shown. The cross (+) represent the magnetic axis. (b) Measured (black) and simulated (red) high-pass-filtered SXR signals for a plasma with a single central structure. Numbers refer to the SXR structure positions in frame (a).

structure is observed when the $(1, 6)$ mode amplitude is substantially higher than all the others. Two structures appear when both the $(1, 6)$ and $(1, 7)$, and in general the other $(m = 1, n)$ modes as well, are significantly decreased in amplitude compared to standard discharges (gray area in Fig. 2).

Description of the single SXR structure signatures illustrates the basic features of the SXR signals, which we will use later to identify the presence of multiple SXR structures. It has already been observed that a sufficiently large, single magnetic perturbation can produce closed helical flux surfaces (a magnetic island) in the plasma core, corresponding to locally enhanced SXR emissivity [7,12]. When the magnetic perturbation rotates, line integrated SXR emissivity oscillates in time, and the spatial pattern and phase relation of the rotating structure is reflected in the data [8]. The oscillation of band-pass-filtered (6 kHz $< f_{\mathrm{SXR}} <$ 70 kHz) SXR signals measured along the lines of sight displayed in Fig. 3(a) are shown in Fig. 3(b). A clear oscillation at $\sim$20 kHz is present in chords A and D, corresponding to off-axis lines of sight with impact parameters $p/a \sim -0.2$ and $\sim$0.4. The impact parameter of a line of sight is its distance from the magnetic axis. The signals from central chords B and C, which correspond to lines of sight passing near the magnetic axis, show more complex features with secondary peaks appearing in a regular sequence. These lower amplitude peaks are superimposed on the oscillation at the dominant frequency.

A comparison of these SXR oscillations with the magnetic perturbation rotation frequency is shown in Fig. 4. The wavelet spectrum [8] for chords A and B is shown in Figs. 4(a) and 4(b), respectively. The spectrum of the SXR signal from chord A shows a strong peak, at a frequency dubbed the *dominant* frequency. The frequency of this peak and its time evolution correspond closely to the rotation frequency of the dominant $(1, 6)$ mode, shown with solid lines in Fig. 4. The wavelet spectrum

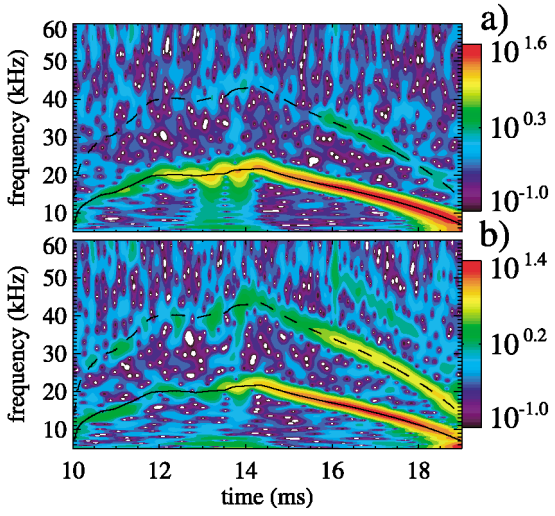

FIG. 4 (color). (a) Wavelet spectra (in arbitrary units) of the SXR signal integrated along line of sight A and (b) line of sight B. Solid lines represent the frequency of the dominant magnetic mode, $f_{1,6}$, while dashed lines represent the first harmonic $2f_{1,6}$.

of chord B, Fig. 4(b), displays peaks at multiples of the dominant frequency. In this particular example, a clear peak in the SXR wavelet occurs at twice the frequency of the (1, 6) magnetic mode, i.e., at the *first harmonic*. The dashed line refers to this magnetic first harmonic. A third peak, at 3 times the rotation frequency of the (1, 6) mode, occasionally appears above the noise level.

These results indicate a poloidally localized pattern in the 2D SXR emissivity, as can be verified by a simulation. The temporally fluctuating SXR emissivity, $\epsilon_{sxr}(r, \theta, t)$, is assumed to arise only from a single poloidally localized, rigidly rotating hot region. The radial and poloidal shape of this region is modeled by Gaussian functions: $\epsilon_{sxr}(r, \theta, t) = \epsilon_0 \cdot e^{-[r-r^\star]^2/\sigma_r^2} \cdot e^{-[\theta-\theta^*(t)]^2/\sigma_\theta^2}$. As the hot region rotates, the poloidal angle $\theta^\star$ varies linearly in time, $\theta^\star(t) = \theta_0 + 2\pi f_{1,6} t$, where $f_{1,6}$ is the rotation frequency of the (1, 6) mode. The amplitude ϵ_0, the radial position $r^\star$, and the widths σ_θ and σ_r are adjusted in order to match the oscillation patterns of Fig. 3(b): for this example, the radial position $r^\star$ corresponds to the resonant radius of the dominant (1, 6) mode, while the radial and poloidal widths are $\sigma_r = 15$ cm and $\sigma_\theta \approx 0.28\pi$, respectively. The filled region in 3(a) represents the contour containing 90% of SXR emissivity of the hot region at time (1). The circle of radius $r^\star$ represents the trajectory of the region. The simulated signals during the rotation periods are represented by the red lines in Fig. 3(b). As shown in Fig. 3(a), this model explains the timing of the numbered peaks in Fig. 3(b). In fact, chords with impact parameter $p > r^\star$ display a single peak, as the structure crosses the chord only once in a rotation period [e.g., position (2) for chord D and position (5) for chord A]. On the other hand, chords with $p < r^\star$ are characterized by two peaks per period, as the region crosses these chords twice per rotation [positions (1) and (3) for chord C and (4), (6) for chord B].

The higher harmonics in the central chords depend on the fact that even if the structure is associated with a magnetic $m = 1$ mode, its poloidal mode decomposition is richer than pure $m = 1$. This may be due to density and temperature gradients into and around the magnetic island and is consistent with results of 3D MHD simulations, which show magnetic modes with $m > 1$, though smaller in amplitude compared to $m = 0$ and $m = 1$ [13].

The strong correlation of the SXR oscillations with the rotation of the dominant magnetic mode suggests that this 2D pattern is the footprint of a helical structure which winds around the torus centered radially on the mode resonant surface. The enhancement of SXR emissivity inside the structure, which has been directly correlated with a local increase of electron temperature in the RFX experiment [12], implies the presence of closed helical flux surfaces, i.e., a magnetic island.

In contrast to the single SXR structure, double SXR structures occur when all of the mode amplitudes decrease. An example is displayed in Fig. 5. Figure 5(a) shows the time traces of the $m = 1, n = 5 - 8$ amplitudes during a discharge in which PPCD is applied from 9 to 16 ms. In this case, all of the modes decrease during PPCD. Figure 5(b) shows the mode rotation frequencies. The (1, 6) and (1, 7) modes rotate at frequencies $f_{1,6}$ and $f_{1,7}$ which are very close, but not identical. The slight difference of the mode frequencies induces a beat pattern in the fluctuating component of the SXR signals, as shown in Fig. 5(c), where the band-pass-filtered SXR signal of chord C is shown. The high frequency corresponds closely to the average frequency of the (1, 6) and (1, 7) modes ($f_{1,6} \sim f_{1,7} \sim 20$ kHz), while the envelope oscillation period corresponds to their frequency difference $\Delta f \sim 1k$ Hz. Figure 5(d) shows the SXR signal from chord C, band-pass-filtered between 30 and 50 kHz, which corresponds to the first harmonic of the magnetic mode frequency. Even in this frequency range a beat pattern is still present. The high frequency component of the oscillation corresponds to twice the dominant frequency, and the envelope oscillation (indicated in the figure by dashed lines) occurs at approximately $\Delta f \sim 2$ kHz. Since SXR oscillations at the first harmonic frequency in central chords imply the presence of a *single*

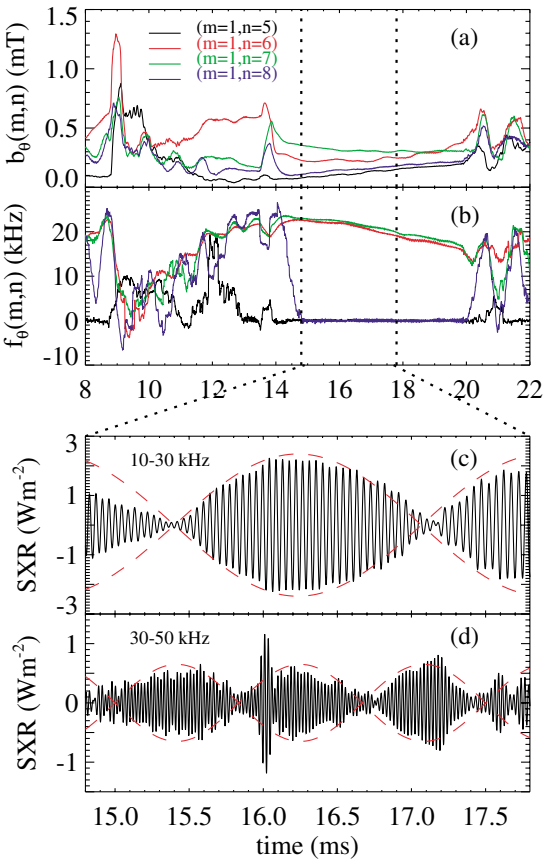

FIG. 5 (color). Magnetic perturbation amplitudes (a) and poloidal rotation frequencies (b). Band-pass-filtered signal of chord C in a frequency range around the dominant frequency (c) and the first harmonic (d).

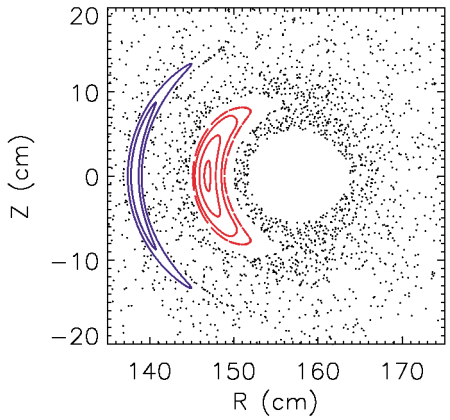

FIG. 6 (color). Poloidal Poincaré plot. The inner island (red) is $m = 1, n = 6$, and the outer one (blue) is $m = 1, n = 7$.

helical structure, the beat at that frequency suggests that now *two* structures are rotating in the plasma core. Moreover, this phenomenon is seen only in central chords with impact parameters near the resonant radii of the (1, 6) and (1, 7) modes. Therefore the SXR helical regions are located near the resonant surfaces of the strongly reduced (1, 6) and (1, 7) modes, and we identify those structures as two marginally nonoverlapped magnetic islands.

In order to verify quantitatively this interpretation, we have mapped individual field line trajectories with the ORBIT code [9], a Hamiltonian guiding center Monte Carlo code, capable of following individual field lines in perturbed magnetic equilibria.

The profiles of the radial magnetic fluctuation $b_{r,(m,n)}(r)$ are computed by solving Newcomb's equation [14], using as boundary conditions the poloidal component of the magnetic fluctuations, $b_{\theta(m,n)}(a)$, measured at the plasma edge. The equilibrium has been computed with a numerical model [1], which uses the experimentally measured toroidal and poloidal field at the edge. All the $b_{r,(m,n)}(r)$ profiles are rescaled by a factor ≈ 0.8. Although there are uncertainties in the modeling, including the dependence of the marginally stable solutions of the Newcomb's equation on the equilibrium fields, the scaling factor has been benchmarked for different plasmas and applies equally well to cases with a single SXR structure.

For the PPCD discharge shown in Fig. 5, the code predicts the presence of two islands with the periodicity of the (1, 6) and (1, 7) modes, in the core of the plasma. This is shown in the poloidal Poincaré plot in Fig. 6.

Note that even if the Chirikov parameter s [15]—defined as the ratio between island sizes and resonant surface distances—is less than 1, the code predicts that magnetic field lines between the two islands are slightly stochastic. This is consistent with theoretical and numerical studies proving that the breaking of the last KAM surface [15] between two resonances occurs for $s < 1$. Nonetheless, the residual level of stochasticity and the diffusivity of magnetic field lines is very low and consistent with the record low value of magnetic fluctuations and the good confinement properties in PPCD [5]. When the normalized magnetic perturbation b is low and approaches the stochastic threshold value b_c, the diffusion decreases like $(b - b_c)^3$ [16]. This is much smaller than the quasilinear diffusion coefficient [17]. Thus, transport is reduced despite the lack of perfect flux surfaces, consistently with the measured increase in energy confinement time, the presence of high-energy electrons [6], the record electron temperature [3], and the dramatic increase in SXR emissivity.

This interpretation explains why double structure features occur in Fig. 2 only when (1, 6) and (1, 7) mode amplitudes are comparable in size and sufficiently low. Double SXR structures are not observed in standard plasmas (shaded region of Fig. 2) because of the large mode amplitudes, corresponding to $s \gg 1$, strong overlap of magnetic island and a highly stochastic field structure with no helical flux surfaces. In conclusion, our data clearly show a change in magnetic topology during PPCD. The appearance of double SXR structures reflect a substantial reduction of magnetic chaos in the plasma core.

The authors acknowledge the technical contributions of I. Molon, G. Gadani, and M. Reyfman and useful discussion with S. C. Prager, J. S. Sarff, and D. Craig.

*Electronic address: http://www.igi.cnr.it/

[1] S. Ortolani and D. D. Schnack, *Magnetohydrodynamics of Plasma Relaxation* (World Scientific, Singapore, 1993).
[2] J. S. Sarff, N. E. Lanier, S. C. Prager, and M. R. Stoneking, Phys. Rev. Lett. **78**, 62 (1997).
[3] B. E. Chapman *et al.*, Phys. Rev. Lett. **87**, 205001 (2001).
[4] R. Bartiromo *et al.*, Phys. Rev. Lett. **82**, 1462 (1999).
[5] J. S. Sarff *et al.*, Nucl. Fusion **43**, 1684 (2003).
[6] R. O'Connell *et al.*, Phys. Rev. Lett. **91**, 045002 (2003).
[7] D. F. Escande *et al.*, Phys. Rev. Lett. **85**, 1662 (2000).
[8] L. Marrelli *et al.*, Phys. Plasmas **9**, 2868 (2002).
[9] R. B. White and M. S. Chance, Phys. Fluids **27**, 2455 (1984).
[10] P. Franz *et al.*, Rev. Sci. Instrum. **74**, 2152 (2003).
[11] R. N. Dexter *et al.*, Fusion Technol. **19**, 131 (1991).
[12] P. Martin *et al.*, Nucl. Fusion **43**, 1855 (2003).
[13] S. Cappello (private communication).
[14] D. C. Robinson, Nucl. Fusion **18**, 939 (1978).
[15] A. J. Lichtenberg and M. A. Lieberman, *Regular and Stochastic Motion* (Springer Verlag, New York, 1983).
[16] R. B. White, *Theory of Toroidally Confined Plasmas* (Imperial College Press, London, 2001).
[17] M. N. Rosenbluth, R. Z. Sagdeev, J. R. Taylor, and G. A. Zaslavsky, Nucl. Fusion **6**, 297 (1966).